

AD-A202 309

OFFICE OF NAVAL RESEARCH

Contract N00014-87-K-0494

R&T Code 400X027YIP

Technical Report No. 1

Diffusional Transport to Nanoscopic Band Electrodes

by

J.D. Seibold, E. R. Scott, and H. S. White

Prepared for Publication in the

Journal of Electroanalytical Chemistry  
(in press)

University of Minnesota  
Department of Chemical Engineering and Materials Science  
Minneapolis, MN 55455

Dec. 5, 1988

Reproduction in whole or in part is permitted for any purpose of the United States Government.

This document has been approved for public release and sale; its distribution is unlimited.

DTIC  
ELECTE  
DEC 12 1988  
S D  
E

## REPORT DOCUMENTATION PAGE

|  |       |  |   |   |          |                             |
|--|-------|--|---|---|----------|-----------------------------|
| 1a. REPORT SECURITY CLASSIFICATION<br><b>Unclassified</b>  |       |  | 1b. RESTRICTIVE MARKINGS  |   |          |                             |
| 2a. SECURITY CLASSIFICATION AUTHORITY  |       |  | 3. DISTRIBUTION / AVAILABILITY OF REPORT<br><br><b>Unclassified/Unlimited</b>   |   |          |                             |
| 2b. DECLASSIFICATION / DOWNGRADING SCHEDULE  |       |  |   |   |          |                             |
| 4. PERFORMING ORGANIZATION REPORT NUMBER(S)<br><br><b>ONR Technical Report 1</b>   |       |  | 5. MONITORING ORGANIZATION REPORT NUMBER(S)   |   |          |                             |
| 5a. NAME OF PERFORMING ORGANIZATION<br><b>Dept of Chemical Engineering<br/>and Materials Science</b>   |       | 5b. OFFICE SYMBOL<br>(If applicable)<br><br><b>Code 1113</b> |   | 7a. NAME OF MONITORING ORGANIZATION<br><br><b>Office of Naval Research</b>                  |          |                             |
| 5c. ADDRESS (City, State, and ZIP Code)<br><br><b>University of Minnesota<br/>Minneapolis, MN 55455</b>  |       |  | 7b. ADDRESS (City, State, and ZIP Code)<br><br><b>800 North Quincy Street<br/>Arlington, VA 22217</b>   |   |          |                             |
| 3a. NAME OF FUNDING / SPONSORING ORGANIZATION<br><b>Office of Naval Research</b>   |       | 3b. OFFICE SYMBOL<br>(If applicable)                         |   | 9. PROCUREMENT INSTRUMENT IDENTIFICATION NUMBER<br><br><b>Contract No. N00014-87-K-0494</b> |          |                             |
| 3c. ADDRESS (City, State, and ZIP Code)<br><br><b>800 North Quincy Street<br/>Arlington, VA 22217-5000</b>   |       |  | 10. SOURCE OF FUNDING NUMBERS   |   |          |                             |
|  |       |  | PROGRAM ELEMENT NO.   | PROJECT NO.   | TASK NO. | WORK UNIT ACCESSION NO.     |
| 11. TITLE (Include Security Classification)<br><br><b>Diffusional Transport to Nanoscopic Band Electrodes</b>  |       |  |   |   |          |                             |
| 12. PERSONAL AUTHOR(S)<br><b>J.D. Seibold, E.R. Scott, and H.S. White</b>  |       |  |   |   |          |                             |
| 13a. TYPE OF REPORT<br><b>Technical</b>  |       | 13b. TIME COVERED<br>FROM _____ TO _____                     |   | 14. DATE OF REPORT (Year, Month, Day)<br><b>December 5, 1988</b>                            |          | 15. PAGE COUNT<br><b>16</b> |
| 16. SUPPLEMENTARY NOTATION   |       |  |   |   |          |                             |
| 17. COSATI CODES   |       |  | 18. SUBJECT TERMS (Continue on reverse if necessary and identify by block number)<br><b>Microelectrodes<sup>*</sup> molecular transport;<br/>interfacial fluid structure . (in figure) ←</b>  |   |          |                             |
| FIELD  | GROUP | SUB-GROUP  |   |   |          |                             |
|  |       |  | 19. ABSTRACT (Continue on reverse if necessary and identify by block number)<br><br><b>Diffusion controlled reactions of electroactive molecules at 20-1000Å wide platinum band electrodes are reported. The reduction of 5,6,11,12-[[Cp*<sub>2</sub>Ru(η-C<sub>6</sub>H<sub>5</sub>)]<sub>4</sub>naphthacene]<sup>4+</sup> and oxidation of Cp*<sub>2</sub>Fe (Cp* = pentamethylcyclopentadienyl) occur at significantly lower rates at electrodes less than 200Å wide than predicted by transport equations based on continuum fluid structure. The results are in qualitative agreement with a recently proposed size-effect theory that accounts for (i) finite dimensions of the reacting molecule and (ii) a decrease in molecular diffusivity near a charged electrode surface. Scanning tunneling microscopy of Pt films used in electrode fabrication indicates an average surface roughness of ca. 10-15Å</b> |   |          |                             |
| 20. DISTRIBUTION / AVAILABILITY OF ABSTRACT<br><input checked="" type="checkbox"/> UNCLASSIFIED/UNLIMITED <input type="checkbox"/> SAME AS RPT <input type="checkbox"/> DTIC USERS |       |  |   | 21. ABSTRACT SECURITY CLASSIFICATION<br><b>Unclassified</b>                                 |          |                             |
| 22a. NAME OF RESPONSIBLE INDIVIDUAL<br><b>Henry S. White</b>   |       |  |   | 22b. TELEPHONE (Include Area Code)<br><b>(612) 625-6995</b>                                 |          | 22c. OFFICE SYMBOL          |

## Diffusional Transport to Nanoscopic Band Electrodes

J. Duke Seibold, Erik R. Scott, and Henry S. White\*  
Department of Chemical Engineering and Materials Science  
University of Minnesota  
Minneapolis, MN 55455

**Abstract.** Diffusion controlled reactions of electroactive molecules at 20-1000Å wide platinum band electrodes are reported. The reduction of 5,6,11,12-[[Cp\*Ru( $\eta$ -C<sub>6</sub>H<sub>5</sub>)]<sub>4</sub>naphthacene]<sup>4+</sup> and oxidation of Cp\*<sub>2</sub>Fe (Cp\* = pentamethylcyclopentadienyl) occur at significantly lower rates at electrodes less than 200 Å wide than predicted by transport equations based on continuum fluid structure. The results are in qualitative agreement with a recently proposed size-effect theory that accounts for (i) finite dimensions of the reacting molecule and (ii) a decrease in molecular diffusivity near a charged electrode surface. Scanning tunneling microscopy of Pt films used in electrode fabrication indicates an average surface roughness of ca. 10-15 Å.



| Accession For                        |   |
|--------------------------------------|---|
| NTIS                                 | GRA&I <input checked="" type="checkbox"/> |
| DTIC                                 | TAB <input type="checkbox"/>              |
| Unannounced <input type="checkbox"/> |   |
| Justification                        |   |
| By _____                             |   |
| Distribution/                        |   |
| Availability Codes                   |   |
| Dist                                 | Avail and/or<br>Special                   |
| A-1                                  |   |

\*To whom correspondence should be addressed.

## Diffusional Transport to Nanoscopic Band Electrodes

J. Duke Seibold, Erik R. Scott, and Henry S. White\*  
Department of Chemical Engineering and Materials Science  
University of Minnesota  
Minneapolis, MN 55455

**Introduction.** Our laboratory recently proposed a heuristic size effect theory to describe electron-transfer reactions at solid Pt band electrodes of molecular widths.<sup>1</sup> The model considers the similar dimensions of electroactive molecule, diffusion length, and interface region (electrical double-layer) at sub-micron electrode structures, yielding qualitative predictions of (i) a breakdown of diffusional transport equations implicitly derived assuming an isotropic continuum fluid structure and (ii) an increased dependence of electrochemical current-voltage characteristics (both kinetic and transport) on near-surface fluid properties, e.g., fluid density and viscosity. The first effect arises as a consequence of the diffusion layer width decreasing at nanoscopic electrodes to values comparable to the dimension of the molecule undergoing reaction. The second effect is a result of molecular transport occurring within an *interfacial* double-layer region with fluid properties which differ considerably from those in the bulk electrolyte. Recent direct measurements of fluid viscosity using surface forces microbalance techniques indicate an increase in viscosity in molecularly thin films of non-polar liquids and aqueous electrolytes trapped between two mica layers<sup>2,3</sup>. Molecular dynamics simulation of local density and diffusivity of liquids contained in pores<sup>4</sup>, at insulating walls<sup>5</sup>, and uncharged metal surfaces<sup>6</sup> support this view.

---

\*To whom correspondence should be addressed.

The effects of near-surface fluid properties on transport rates should be more pronounced at nanoscopic electrodes than at conventionally sized electrodes due to the decrease in diffusion layer width that accompanies reduction of the electrode size. Preliminary experimental work in our laboratory<sup>1</sup> and others<sup>7</sup> has demonstrated a correlation of transport limited currents with the Pt band width that deviates strongly from classical diffusion equations. For instance, the transport limited electrooxidation of ferrocene<sup>1</sup> and ferrocyanide,<sup>7</sup> at platinum band electrodes of widths less than 200Å occur at a rate ca. 3-5 times slower than predicted by continuum based transport equations. The dependence of limiting currents on molecule size is in qualitative agreement with predictions of our model. Recently, we have also experimentally demonstrated a dependence of the limiting current on the solution ionic strength that is specific to nanoscopic electrodes<sup>8</sup>, suggesting an influence of the electrical double-layer on near surface transport at electrodes of submicron dimension. In this report, we describe new measurements of transport limited currents observed at 20 to 1000Å wide Pt band electrodes. The results are in agreement with previous results indicating a decrease in molecular diffusivity within molecular distances of the electrode surface. Preliminary results from scanning tunneling microscopy of the Pt thin films used in electrode preparation are also described in this report.

## **Experimental.**

*Metal Films and Electrode Preparation.* Pt films, 20 to 1000Å thick, were deposited on cleaved mica by r.f. ion sputtering. Film thicknesses of 20 to 100Å thick films were measured by ellipsometry and found to agree within 20% of the mass average value. A detailed description of metal film preparation and characterization has been described previously<sup>9,10</sup>. Measurements of metal film continuity and topography using scanning tunneling microscopy are described in the Results and Discussion section. Electrical contact to the Pt film was made by attaching a fine wire using Ag paint. The Pt films were

placed in an inverted rubber septum used as a cylindrical mold and filled with epoxy (Magen Scientific Inc., Cm-161 resin and hardener). The epoxy was allowed to dry 24 hours before removing the mold. A 6 cm glass tube was utilized as a conduit for the fine wire and sealed with epoxy. The encapsulated mica/Pt structure was ground flat perpendicular to the film exposing electrodes of band geometry, ca. 1 cm long and 20-1000 Å wide. Wheel grinding with silicon carbide 320 grit followed by 600 grit yielded the most reproducible measurements of limiting current. Polishing with 1200 grit sand paper or with 0.05 μ alumina led to poor reproducibility and significantly smaller limiting currents.

The electrical resistivity of the Pt films used in this study is slightly dependent on the film thickness, ranging from  $4 \times 10^{-5}$  to  $1.1 \times 10^{-4}$  ohm-cm for 500 and 20 Å thick films, respectively. Based on the film geometry and magnitude of currents observed at these electrodes, the ohmic potential drop within the film is less than 1 mV for all reported experimental measurements.

*Instrumentation and Chemicals.* A standard three-electrode electrochemical cell was used throughout. The counter and reference electrodes were Pt and oxide coated Ag wires, respectively. Cyclic voltammograms were obtained using a Princeton Applied Research Model 173 potentiostat and 175 programmer.

Tetrabutylammonium perchlorate (TBAP) was recrystallized from acetone/ether, dried at 80 °C and stored under vacuum at 50 °C. Acetonitrile (spec. grade) was stored over molecular sieves. Bis(pentamethylcyclopentadienyl)iron (Strem Chem.) and 5,6,11,12-tetra[(pentamethylcyclopentadienyl)ruthenium(η-phenyl)]naphthalene hexafluorophosphate ((Cp\*<sub>2</sub>Ru(η-C<sub>6</sub>H<sub>5</sub>))<sub>2</sub>C<sub>10</sub>H<sub>8</sub>)(PF<sub>6</sub>)<sub>4</sub>) were used as received. The sample of ((Cp\*<sub>2</sub>Ru(η-C<sub>6</sub>H<sub>5</sub>))<sub>2</sub>C<sub>10</sub>H<sub>8</sub>)(PF<sub>6</sub>)<sub>4</sub> was a gift from Drs. M.D. Ward and P. J. Fagan of E. I. Dupont de Nemours & Co<sup>11</sup>. STM images of Pt films were obtained using

a Nanoscope II Scanning tunneling microscope (Digital Instruments, Santa Barbara, CA). A detailed STM study of these metal films is to be reported elsewhere<sup>12</sup>.

**Results and Discussion.** Fig. 1 shows voltammograms obtained at a nominally 60 Å wide x 1cm long Pt band electrode corresponding to the 1-e<sup>-</sup> oxidation of bis(decamethylcyclopentadienyl)iron (Cp\*<sub>2</sub>Fe) and the 1-e<sup>-</sup> reduction of (Cp\*<sub>2</sub>Ru(η-C<sub>6</sub>H<sub>5</sub>))<sub>4</sub>C<sub>14</sub>H<sub>6</sub><sup>+4</sup>. Both redox molecules were present at millimolar concentrations (typically 2 mM) in an unstirred acetonitrile solution containing 0.1M tetra(n-butyl)ammonium perchlorate (TBAP) as supporting electrolyte and purged thoroughly with N<sub>2</sub>. The sigmoidal shaped voltammograms shown in Fig. 1 are characteristic of one (or more) electrode dimension significantly smaller than the depletion layer thickness established by diffusion controlled oxidation or reduction at the electrode surface.<sup>13</sup>

Voltammetric measurements were made for the oxidation of Cp\*<sub>2</sub>Fe and reduction of (Cp\*<sub>2</sub>Ru(η-C<sub>6</sub>H<sub>5</sub>))<sub>4</sub>C<sub>14</sub>H<sub>6</sub><sup>+4</sup> at electrodes of widths between 20 and 1000 Å. Qualitatively the voltammograms at all electrodes have similar waveshape to those shown in Fig 1. However, voltammetric curves generally appeared less reversible for electrodes less than 60 Å wide, indicating the onset of heterogeneous kinetic limitations at the smaller electrodes. As discussed in the experimental section, the shapes of the voltammograms and limiting currents are not effected by the electrical resistance of the metal film, which generates an internal potential loss of less than 1 mV in all cases.

The potential independent limiting current,  $i_{lim}$ , is a measure of the molecular flux to the electrode surface when the surface concentration is depleted to a near zero value. Assuming a hemicylindrical electrode, the long-time limit of the radial flux to the surface is given by<sup>14</sup>

$$i(t) = \frac{2nFDIC^b\pi}{\ln[4Dt/r_0^2]} \quad \text{eq. 1}$$

where  $D$  is the diffusivity of the reacting molecule in the bulk solution,  $F$  is the Faraday,  $l$  is the electrode length,  $t$  is time, and  $r_0$  is the *effective* hemicylindrical electrode radius. Several reports have shown that eq. 1 accurately predicts quasi-steady-state limiting currents observed at band electrodes of width  $w$  between  $500\text{\AA}$  and several microns, when the effective radius is assumed to be equal to  $w/\pi$ <sup>15</sup>. A more recent theoretical treatment by Szabo et. al.<sup>16</sup> indicates that eq. 1 exactly describes the current response at band electrodes if  $w/4$  is substituted for  $r_0$ . For submicron wide band electrodes and at long times, however, the difference in the current predicted by eq. 1 using either  $w/4$  or  $w/\pi$  is very small. For instance, using  $D = 10^{-5} \text{ cm}^2/\text{s}$ ,  $t = 25 \text{ s}$ , and  $w = 500\text{\AA}$ , the limiting current predicted by eq. 1 is ca. 2 % larger than when using  $w/\pi$  as the effective radius. In view of this small difference and the significant scatter in experimental data, we have chosen to use eq. 1 with an effective radius,  $r_0$ , equal to  $w/\pi$  to allow for direct comparison with our early studies.

Normalized limiting currents ( $i/2nFDlC^b\pi$ ) obtained for  $\text{Cp}_2^*\text{Fe}$  oxidation and  $(\text{Cp}^*\text{Ru}(\eta\text{-C}_6\text{H}_5))_4\text{C}_{14}\text{H}_6^{+4}$  reduction are plotted in Fig. 2 versus the effective normalized electrode width ( $1/\ln(4Dt/r_0^2)$ ). The solid line in Fig. 2 represents eq. 1, the theoretical flux based on a continuum fluid. Diffusivities of  $1.2 \pm 0.5 \cdot 10^{-5}$  and  $2.2 \pm 0.5 \cdot 10^{-5} \text{ cm}^2/\text{s}$  for  $(\text{Cp}^*\text{Ru}(\eta\text{-C}_6\text{H}_5))_4\text{C}_{14}\text{H}_6^{+4}$  and  $\text{Cp}^*\text{Fe}$ , respectively, were obtained from the steady-state limiting current at  $25 \mu\text{m}$  Pt disks, and are used in plotting experimental points in Fig. 2. A value of  $t = 25 \text{ s}$  was used in calculating  $Dt/r_0^2$ , corresponding to the time required to scan the potential over a  $0.5 \text{ V}$  range at  $20 \text{ mv/s}$ . Each point in Fig. 2 represents a set of 6-12 independent measurements using different electrodes.

Fig. 2 shows that the limiting currents observed at  $500$  and  $1000 \text{\AA}$  wide electrodes are within error of predicted values using eq. 1. Beginning with electrodes of  $200 \text{\AA}$  width, normalized limiting currents deviate strongly from the expected diffusional flux. A

similar experimental trend is observed for the oxidation of ferrocyanide in H<sub>2</sub>O and ferrocene in acetonitrile.

Eq. 1 is derived assuming a continuum fluid structure and a constant valued diffusivity. Both assumptions are implicitly contained in transport equations describing *i*-*V* characteristics in homogeneous fluids. In the previous report we argued that the diffusional flux equations based on the continuum fluid model are inconsistent with physical expectations for non-planar electrodes of submicron dimensions. The bases for this argument are two-fold. First, the finite size of the reacting species limits its distance of approach to the electrode surface. At nanoscopic spherical and cylindrical (or band) electrodes, a significant variation in the predicted reactant concentration, based on continuum flux equations, occurs within molecular distances of the electrode surface. As a result the predicted concentration profile can no longer be described by a continuous curve originating at the surface. To account for this, we have proposed that the surface concentration of redox active species used to calculate the flux (*viz.* eq. 1) is better described by an average concentration based on the instantaneous number of redox molecules, *N*, contained within a hypothetical reaction zone of thickness corresponding to the diameter (*2z*) of the reacting species (typically of the order of 1 nm). For large electrodes, where the flux is relatively small, *N* approaches zero for reactions occurring on the limiting current plateau. Second, we have considered the effect of fluid inhomogeneity within the interphase resulting from the presence of a hard, highly charged metal wall. We have previously proposed that non-bulk properties of the electrolyte layer in immediate contact with the surface will decrease the effective diffusional flux of reactant to the surface, resulting in a lower limiting current. The thickness of this non-bulk layer is expected to be of the thickness of several solvent diameters, again typically of the order of 1 nm.

The above mentioned concepts have been incorporated into a heuristic size effect model to yield the surface redox concentration:

$$C(r_0 < r < z) = C(r \rightarrow \infty) [8\zeta / ((1 + r_0/z) \ln(4Dt/r_0^2))] ]$$

which has a non-zero for values of  $r_0$  less than  $0.1 \mu\text{m}$ . Applying this surface concentration as a first order correction to the continuum based flux equation, eq. 1, yields:

$$i(t) = 2nFIDC^b\pi \left( \frac{(1 + r_0/z)(\ln(4Dt/r_0^2) - 8\zeta)}{(1 + r_0/z)\ln^2(4Dt/r_0^2)} \right) \quad \text{eq. 2}$$

Here  $2z$  represents the thickness of the interfacial reaction layer at the electrode surface,  $\zeta$  is the ratio of diffusion coefficient in the bulk relative to that near the electrode surface,  $D_{\text{bulk}}/D_{\text{surf}}$ , which accounts for changes in fluid properties in the reaction layer. Note that, in the limit  $r_0/z \rightarrow \infty$ , eq. 2 reduces to eq. 1, corresponding to the behavior of macroscopic electrodes.\*

In analyzing the data of Figure 2, we have used  $z = 12 \text{ \AA}$  and an average value of  $1.7 \cdot 10^{-5} \text{ cm}^2/\text{s}$  for the bulk diffusivity of the two test molecules. The resulting analysis provides an estimate of the parameter,  $\zeta$ , using eq. 2 to fit the data in Fig. 2. Our choice of  $z$  is somewhat arbitrary, but has been chosen to be of the same magnitude as the size of the reacting species ( $2z = 7 \text{ \AA}$  for  $\text{Cp}_2^*\text{Fe}$  and  $2z = 18 \text{ \AA}$  for  $([\text{Cp}^*\text{Ru}(\eta\text{-C}_6\text{H}_5)]_4\text{naphthacene}^{4+})$ ).

The dashed line shown in Fig. 2 is a plot of eq. 2 using  $\zeta = 6$ . However, values of  $\zeta$  in the range 3 – 9 also yielded theoretical curves that passed through a majority of data in Fig. 2 (within one std. deviation). This range is similar to that previously observed from the analysis of limiting currents for ferrocene oxidation in acetonitrile and ferrocyanide in

\*In ref. 1, the factor of 2 in  $(2nFIDC^b\pi)$  was omitted in equations corresponding to eqs. 1 and 2 of the present text. Since both experimental and theoretical points were normalized by the same group of constants, this omission did not affect the quantitative agreement between reported data and theory. We thank a reviewer for pointing out this error.

water ( $\zeta = 3-5$ ). The experimental results suggest a substantial change in the effective diffusivity within molecular distances of the surface. However, the model employed in the analysis, which is based on a step-wise change in diffusivity at a distance  $2z$ , probably overestimates of the effect of fluid inhomogeneity at the surface. A more realistic picture of the fluid inhomogeneity is contained in the results of Chan and Horn<sup>2</sup>, who measured the viscosity of nonpolar (no electrolyte) fluids using surface forces microbalance techniques. In these experiments, the effective viscosity of fluids between two crossed mica cylinders was measured as the cylinders were squeezed from long distances to contact. Their results indicate a significant increase in effective fluid viscosity relative to the bulk value at distances ranging from contact to several hundred angstroms. In the fluid region within 1 nm of the surface, they observed a step-wise flow of solvent resulting from solvation forces. The complex flow in the experiments of Chan and Horn do not allow a direct measurement of the local microscopic viscosity required in our analysis, but do point out the complex structure of the solvent not accounted for in our analysis. In addition, strong electrostatic forces and ion adsorption, neither of which are included in the present model, may have a significant effect on transport limited rates at nanoscopic electrode substrates. We are currently working toward an understanding of these factors.

*Topography and Continuity of Pt Thin Films on Mica.* A difficult issue to address when working with submicron electrodes concerns characterization of the electrode area exposed to the electrolyte. The roughness and continuity of the sputtered deposited Pt films, prior to mounting in insulating phase, inherently limits the degree to which rectangular band geometries can be obtained. Grinding or cutting the metal encapsulated films to obtain a band geometry creates further uncertainties about the true geometry of the exposed surface. As discussed in the previous report, we believe that the grinding procedure used in our lab, which yields the most reproducible measurements, is the major source of error in the limiting current values and in the determination of  $\zeta$ . However, the general trend shown in

Fig. 2 has been observed in our laboratory using different polishing procedures and by others employing different encapsulating materials.

Deposition of metals onto freshly cleaved mica does not, in general, lead to continuous flat films. For instance, deposition of Au onto mica by thermal evaporation yields islands for mass quantities of Au that ideally would correspond to moderately thin films ( $\sim 100 \text{ \AA}$ ). The deposition of Ag onto mica by evaporation yields crystalline films that contain microscopic voids. Band electrodes prepared by deposition of Au or Ag onto mica would not be expected have a continuous and/or uniform area exposed to solution. Transmission electron microscopy (TEM) of Pt films on mica has shown that these thin films are continuous and polycrystalline with an average grain diameter of  $\sim 50 \text{ \AA}$ . However it has proven difficult of obtain a direct and quantitative measurement of the microscopic roughness of these films. In regard to band electrode studies, a continuous but rough surface would yield electrodes that may be better described by a series of irregular nanoscopic metal disk electrodes interconnected by thinner metal strips.

Scanning tunneling microscopy (STM) was used to obtain topographical images of the Pt films in order to access the continuity and roughness. STM of thick Pt films ( $1.8 \text{ \mu m}$ ) on mica have also been reported by Fan and Bard,<sup>17</sup> which show large surface regions that are nearly atomically smooth. The images reported here, however, show detailed structure not observed in this earlier work, which may be due to the large difference in film thickness and to the deposition procedure. Fig. 3 shows two representative images recorded of 40 and 200  $\text{\AA}$  Pt thick films. The 40  $\text{\AA}$  thick film (Fig. 3a) appears very structured, with rolling hills spaced ca. 50-100  $\text{\AA}$  apart. The peak-to-valley vertical dimensions are typically about 10  $\text{\AA}$ , although larger features have been occasionally observed. In contrast, STM images of films of thickness between 60 and 500  $\text{\AA}$  clearly and reproducibly show the presence of individual metal grains of the film. The size and shape of these grains observed in STM images are in qualitative agreement with previous TEM images of 60 $\text{\AA}$  films. For Pt films thicker than 500 $\text{\AA}$ , the topography

gradually varies from the relatively smooth surface of the polycrystalline surfaces shown in Fig. 3b, to a surface with peak-to-valley dimensions of  $\sim 30 - 100 \text{ \AA}$ .

The STM images clearly show that the Pt films are microscopically rough and that the topography depends strongly on the film thickness. Band electrodes prepared from these films will have variations in width along the length of the electrode. However, from STM images, we estimate that the thickness should not vary by more than 30 - 40 % (corresponding to  $15 \text{ \AA}$  roughness on a  $40 \text{ \AA}$  film). This value is in agreement with previous electrical resistivity and surface forces measurements<sup>9</sup>, both of which indicate that  $40 \text{ \AA}$  films have an average roughness of  $\sim 10 \text{ \AA}$  or less.

The small amplitude roughness may affect the limiting current values at these electrodes, but we expect this discrepancy to be small and probably insignificant. We note that the limiting currents for the band geometry is predicted from the classical diffusion equation to be quite insensitive to the band thickness. The magnitude of the limiting current, for example, is expected to decrease by only 7.2% as the electrode width is reduced from 100 to  $40 \text{ \AA}$ . Thus, it is probably not likely that the effects of the observed topographical features would have a discernable effect on the voltammetric behavior of these electrodes.

**Conclusion.** The experimental results described here support the previously proposed model of size effects occurring at nanoscopic band electrodes. Qualitatively, the magnitude of the limiting currents deviates strongly from the classical theoretical predictions at electrodes  $< 200 \text{ \AA}$ , a consequence of the finite size of the reacting molecule and a near-surface transport rate that is significantly smaller than in the bulk electrolyte. Quantitatively, the deviation of limiting current is considerably larger than anticipated based on direct experimental measurements of near-surface fluid viscosity and molecular dynamics simulations of fluid structure near a hard-wall. This discrepancy is in part, due to limitations of the size-effect model in realistically describing fluid properties near the

electrode surface. Imperfections in the electrode geometry, partially revealed by STM images of Pt films prior to electrode fabrication, probably have a small effect on the electrode response. Both issues are currently being addressed in our laboratory.

**Acknowledgement.** This work was support by the Office of Naval Research.

### Figure Captions.

1. Cyclic voltammograms corresponding to the oxidation of 2.0 mM Cp\*<sub>2</sub>Fe and the reduction of 2.0 mM (Cp\*<sub>2</sub>Ru(η-C<sub>6</sub>H<sub>5</sub>))<sub>4</sub>C<sub>14</sub>H<sub>6</sub><sup>+4</sup> in acetonitrile containing 0.1 M TBAP as supporting electrolyte. Scan rate = 20 mV/s. Solutions purged with N<sub>2</sub>.

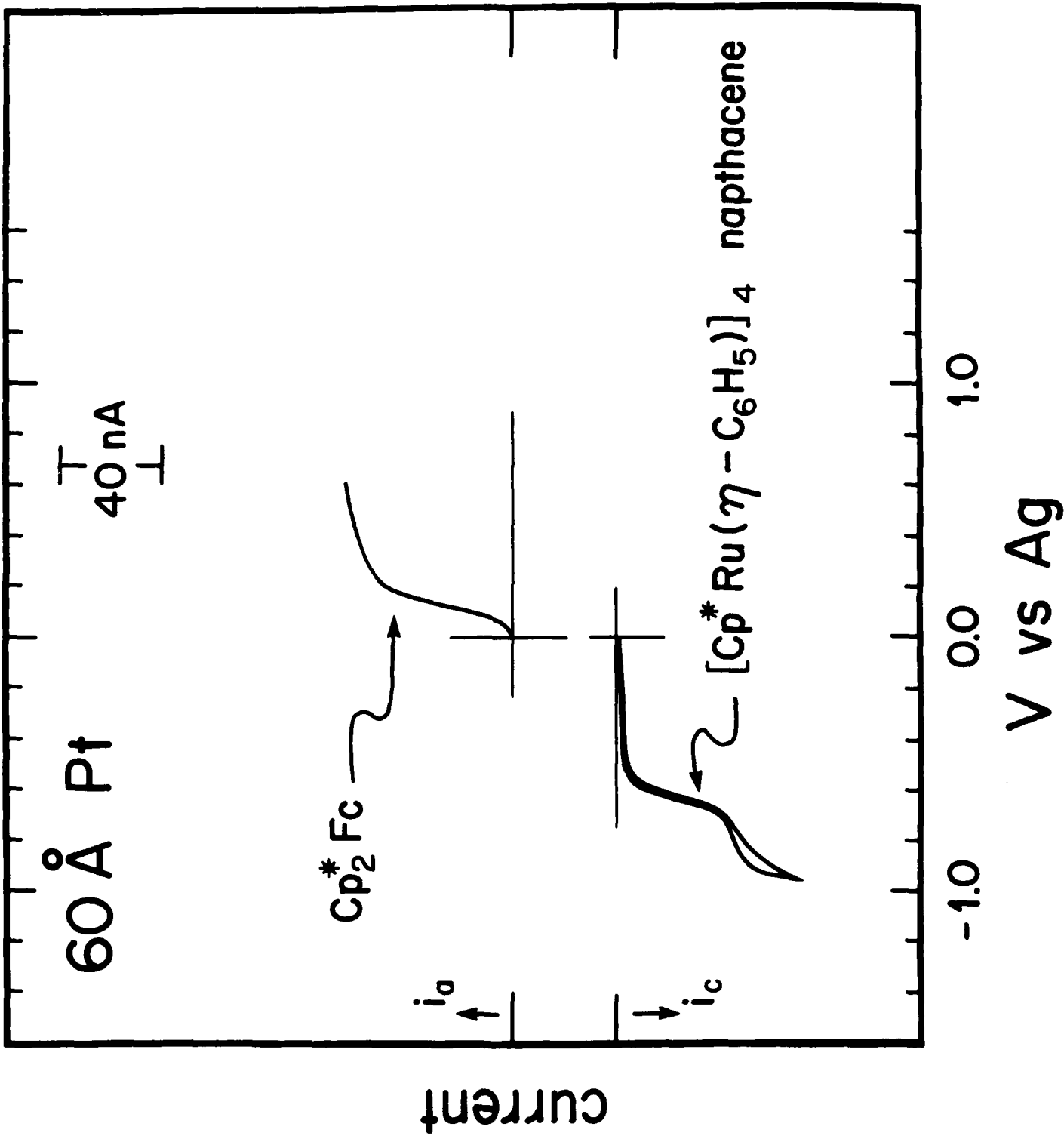
2. Plot of normalized limiting current ( $i/2nFIDC^b\pi$ ) vs  $\{\ln[4Dt/r_0^2]\}^{-1}$  obtained for the oxidation of Cp\*<sub>2</sub>Fe and the reduction of (Cp\*<sub>2</sub>Ru(η-C<sub>6</sub>H<sub>5</sub>))<sub>4</sub>C<sub>14</sub>H<sub>6</sub><sup>+4</sup> in acetonitrile containing 0.1 M TBAP as supporting electrolyte. The solid line corresponds to eq. 1, the response expected for diffusional transport to a hemicylindrical electrode. The dashed line represents the fit of eq. 2 to the experimental data using  $z = 12\text{\AA}$  and  $\zeta = 6$ . Electrode widths are indicated on the plot. The error bars represent one standard deviation from the mean value. Each data point represents the mean of a minimum of 6 independent measurements.

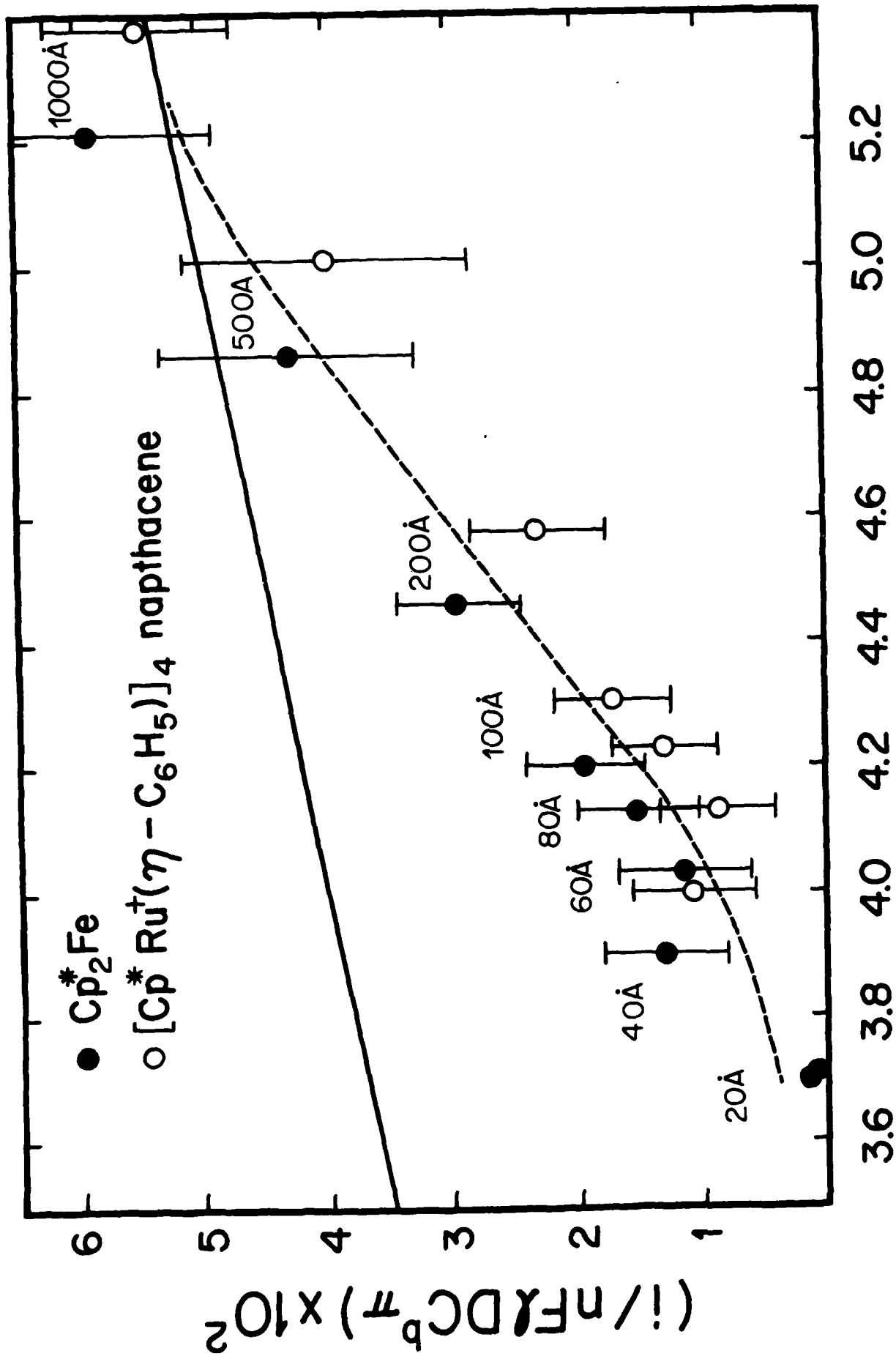
3. Scanning tunneling microscopy images of (a) 40 and (b) 200Å thick Pt films prior to electrode fabrication. Images were taken in constant current mode. Tunneling current = 0.5 nA, sample/tip bias = 50 mV.

## References.

---

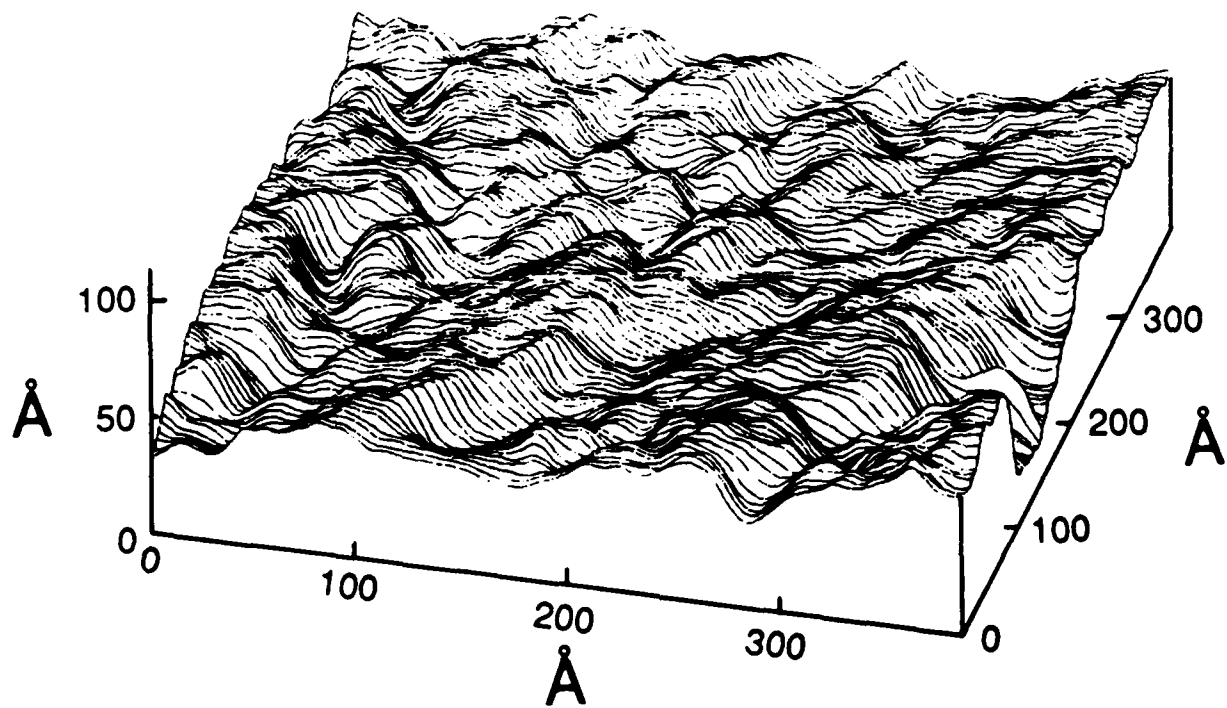
1. R.B. Morris, D.J. Franta, and H. S. White, J. Phys. Chem., **91**, (1987), 3559.
2. D.Y.C. Chan and R.G.Horn, J. Chem. Phys., **83**(10), (1985), 5311.
3. J. N. Israelachvili, J. Coll. Int. Sci., **110**, (1986), 263.
4. J.J. Magda, M. Tirrell, , H.T. Davis, J. Phys. Chem., **83**, (1985),1888.
5. A.A. Gardner and J. P. Valleau, J. Chem. Phys., **86**, (1987), 4171.
6. J. P. Valleau and A.A. Gardner, J. Chem. Phys., **86**, (1987), 4162.
7. K. Wehmeyer, M.R. Deakin, R. M. Wightman, Anal. Chem. **57**, (1985) 1913.
8. J. D. Norton, J.D. Seibold, and H. S. White, in preparation.
9. C. P. Smith, M. Maeda, Lj. Atanoska, H.S. White, and D.J. McClure, J. Phys. Chem.,**92**, (1988)199.
10. M. Maeda, H. S. White, and D. J. McClure, J.Electroanal. Chem., **200** (1986) 383.
11. P.J. Fagan, M. D. Ward, J.V. Caspar, J. C. Calabrese, and P.J. Krusic, J. Am. Chem. Soc., **110** (1988) 2981.
12. E.R. Scott, H.S. White, D.J. McClure, J. Phys. Chem., submitted (1988).
13. R. M. Wightman, Anal. Chem. **53**, (1981) 1125A.
14. J.C. Jaegar, Proc. R. Soc. Edinburgh, **A61**, (1942), 223
15. P. M. Kovach, W. L. Caudill, D. G. Peters, R. M. Wightman, Electroanal. Chem., **185**, (1985), 285.
16. A. Szabo, D. K. Cope, D. E. Tallman, P. M. Kovach, and R. M. Wrightman, J. Electroanal. Chem., **217** (1987) 417.
17. F.-R. F. Fan and A.J. Bard, Anal. Chem., **60** (1988), 751 .





$$1/\ln[4Dt/r_0^2] \times 10^2$$

A. 40Å Pt



B. 200Å Pt

